SCIENCE CHINA
Technological Sciences

October 2012 Vol.55 No.10: 2750–2756
doi: 10.1007/s11431-012-4913-7

Theoretical development for DSMC local time stepping technique

CAI GuoBiao[1*], SU Wei[1] & HOU FengLong[2]

[1] *School of Astronautics, Beihang University, Beijing 100191, China;*
[2] *Chinese Academy of Space Technology, Beijing 100049, China*

Received September 23, 2011; accepted March 9, 2012; published online July 4, 2012

The direct simulation Monte Carlo (DSMC) method is the most mature and wildly used approach for nonequilibrium gas flow simulation. The phenomenological nature of this method brings flexibility to the computation algorithms. In this study, the theoretical foundations to decouple the molecular motion and collision within a time step are discussed in detail, which can be treated as criterions for the DSMC algorithms. Based on the theoretical developments, an improved local time stepping scheme is proposed, which specifies the movement time attribute and the collision time attribute for each representative particle. A free flow about a sphere body is considered as an example, which is compared with the calculations using the published local time stepping technique. The results show that the improved local time scheme is valid and is promising in realizing flow structures with strong variations.

DSMC method, local time step, movement time attribute, collision time attribute

Citation: Cai G B, Su W, Hou F L. Theoretical development for DSMC local time stepping technique. Sci China Tech Sci, 2012, 55: 2750–2756, doi: 10.1007/s11431-012-4913-7

1 Introduction

The most mature and wildly used approach to simulate the nonequilibrium gas flows is the direct simulation Monte Carlo (DSMC) method, which was developed in the early 1960s [1] and has been successfully applied to a wide range of rarefied gas dynamics problems. In general, the DSMC method computes the gas flow through simulating the random evolvement of the simulated particle system. The velocities of the particles represent the gas velocity distributions and the macroscopic properties of the flow are obtained by averaging the properties of the representative particles. The random evolvement of the system is performed by directly simulating the motions and collisions of the particles. In a real gas flow, the molecular motions, collisions and surface interactions deeply couple with each other. In order to simplify the procedure, molecular motion and collision are decoupled during a small time interval that is required to be as small as the local mean collision time. Within the time step, the particles move through the computational grid and interact with the boundary surfaces firstly. Then, the probable collisions of each particle over the time interval are simulated following phenomenological molecular interaction models, and the particle velocities and other properties are updated except the positions which are unchanged in collision treatment.

Although, the DSMC method is a mature approach to dilute gas simulations, the physical nature of the DSMC method, which requires resolution of the mean free path and the collision rates by appropriate cell sizes and simulation time steps, leads to the high computational expense. A large number of approaches have been used to reduce the computational

*Corresponding author (email: cgb@buaa.edu.cn)

expense, such as grid adaption, parallelization, and local time stepping technique. The technique utilizing a local time step with automatic adaption is implemented when the macroscopic gradients and the local mean collision frequencies vary within wide limits. A lot of research works have been published to discuss this strategy. In the published DSMC simulation software named DSMC Analysis Code (DAC), a local time step is assigned to each grid cell and can be regulated during computations [2, 3]. In the year of 1998, M. S. Ivanov divided the computational domain into several sub domains, and assigned a different time step to each sub domain [4]. This local time stepping technique was performed in famous DSMC simulation software named Statistical Modeling in Low-density Environment (SMILE). In the same year, Laux M. used a discrete cell-local time step with automatic adaption to develop flow field [5]. In the year of 2001, Teshima K implemented the local time step scheme, which was in a similar way performed in SMILE to calculate the supersonic expansion at a very large pressure ratio [6]. Then in the year of 2005, the DS3V DSMC simulation software was developed and a local time step technology was applied [7].

All the research works listed above are mainly focused on the local time stepping technique. However, the implementations of this strategy vary a lot in details. This study intends to explain the theoretical foundations of the local time step technique and propose an improved local time stepping scheme. The remainder of this paper is organized as follows. Firstly, the foundations of decoupling molecular motion and collision are discussed. Based on the theoretical discussion, an improved local time step scheme to specify the movement time interval and the collision time interval for each representative particle is proposed. Then, the scheme is tested using a hypersonic flow over a three-dimensional sphere. Finally, the paper ends with some concluding remarks.

2 Theoretical discussion

It is well known that the DSMC method is equivalent to solving the Boltzmann equation. The Boltzmann equation is the governing equation for dilute gas flow, which indicates the relationship between the velocity distribution functions and the variables on which they depend [1]. This function is deduced following the assumptions of molecular chaos and binary intermolecular collisions, which has the form [8]:

$$\frac{\partial f}{\partial t} = -\boldsymbol{c}\cdot\frac{\partial f}{\partial \boldsymbol{r}} - \boldsymbol{F}\cdot\frac{\partial f}{\partial \boldsymbol{c}} + \int_{-\infty}^{\infty}\int_{0}^{4\pi}(f^{'}f_1^{'} - f\ f_1)c_r\sigma \mathrm{d}\Omega \mathrm{d}\boldsymbol{c}_1. \quad (1)$$

The velocity-distribution function f is defined as follows: $f(t,\boldsymbol{r},\boldsymbol{c})\mathrm{d}\boldsymbol{r}\mathrm{d}\boldsymbol{c}$ is the number of molecules, at time instant t, with velocity components lying within the limits $\boldsymbol{c}$ and $\boldsymbol{c}+\mathrm{d}\boldsymbol{c}$, and spatial components lying within the limits $\boldsymbol{r}$ and $\boldsymbol{r}+\mathrm{d}\boldsymbol{r}$. To consider the item $-\boldsymbol{c}\cdot(\partial f/\partial \boldsymbol{r})$ and $-\boldsymbol{F}\cdot(\partial f/\partial \boldsymbol{c})$, the generations of numbers of molecules caused by the flux across the various side-surfaces of the spatial volume $\mathrm{d}\boldsymbol{r}$ and velocity volume $\mathrm{d}\boldsymbol{c}$ during the time interval $\mathrm{d}t$ are respectively equal to $-\boldsymbol{c}\cdot(\partial f/\partial \boldsymbol{r})\mathrm{d}\boldsymbol{c}\mathrm{d}\boldsymbol{r}\mathrm{d}t$ and $-\boldsymbol{F}\cdot(\partial f/\partial \boldsymbol{c})\mathrm{d}\boldsymbol{c}\mathrm{d}\boldsymbol{r}\mathrm{d}t$. Whereas the last item of the right side of the equation exactly represents the change of the molecules per unit phase-volume and per unit time as the consequence of the collisions.

In DSMC simulation, the particle motion and collision are decoupled within a small time interval. This decoupling process can be easily explained through the Boltzmann equation. For the sake of simplicity, two operators Df and Jf are used to denote [9]

$$Df = \boldsymbol{c}\cdot\frac{\partial f}{\partial \boldsymbol{r}} + \boldsymbol{F}\cdot\frac{\partial f}{\partial \boldsymbol{c}}, \quad (2)$$

$$Jf = \int_{-\infty}^{\infty}\int_{0}^{4\pi}(f'f_1' - f\ f_1)c_r\sigma \mathrm{d}\Omega \mathrm{d}\boldsymbol{c}_1. \quad (3)$$

Then, the Boltzmann equation becomes

$$\frac{\partial f}{\partial t} = -Df + Jf. \quad (4)$$

According to the Taylor expansion theory, the velocity-distribution function can be expressed as

$$\begin{aligned} f(\boldsymbol{c},\boldsymbol{r},t+\Delta t) &= f(\boldsymbol{c},\boldsymbol{r},t) + \left[\frac{\partial f(\boldsymbol{c},\boldsymbol{r},t)}{\partial t}\right]_t \Delta t + O[(\Delta t)^2] \\ &= (1-\Delta tD+\Delta tJ)f(\boldsymbol{c},\boldsymbol{r},t) + O[(\Delta t)^2]. \end{aligned} \quad (5)$$

By adding the second-order operator $(\Delta t)^2D(Jf)$ to the right side of the equation, the velocity-distribution function can be written as

$$f(\boldsymbol{c},\boldsymbol{r},t+\Delta t) = (1+\Delta tJ)(1-\Delta tD)f(\boldsymbol{c},\boldsymbol{r},t) + O[(\Delta t)^2], \quad (6)$$

and to neglect the second-order error term, it can be expressed step by step as

$$f_D(\boldsymbol{c},\boldsymbol{r},t+\Delta t) = (1-\Delta tD)f(\boldsymbol{c},\boldsymbol{r},t), \quad (7)$$

$$f(\boldsymbol{c},\boldsymbol{r},t+\Delta t) = (1-\Delta tJ)f_D(\boldsymbol{c},\boldsymbol{r},t+\Delta t). \quad (8)$$

$f_D(\boldsymbol{c},\boldsymbol{r},t+\Delta t)$ is the velocity-distribution function at time instant $t+\Delta t$, if the collision effect is negligible. On the base of $f_D(\boldsymbol{c},\boldsymbol{r},t+\Delta t)$, $(1-\Delta tJ)\ f_D(\boldsymbol{c},\boldsymbol{r},t+\Delta t)$ is the final velocity distribution function including the effect of molecular collision.

Eqs. (5) and (6) show that the molecular motion and collision can be decoupled, and the numerical error brought by the decoupling process is just as small as the quantity $(\Delta t)^2$. Hence, the DSMC process is of the first-order accuracy in time. Furthermore, the velocity-distribution function is also written as

$$f(\boldsymbol{c},\boldsymbol{r},t+\Delta t) = (1-\Delta tD)(1+\Delta tJ)f(\boldsymbol{c},\boldsymbol{r},t) + O[(\Delta t)^2]. \quad (9)$$

It means that the sequence of molecular motion and colli-

sion treatments is not important. To enforce the particles colliding prior to moving can get the same results.

In the DSMC method, the simulating period of the simulation system is consistent with the time of the real gas flows. The particles evolving from t_0 to t_l demonstrates that the gas flow develops from t_0 to t_l (the subscript l is the index of time series). Since the random evolvement of particles includes molecular motions and collisions, two different time attributes, movement time attribute t_m and collision time attribute t_c, might be assigned to each representative particle. When the motion is treated within the time interval t_l to t_{l+1} the particle movement time attribute $t_{m,l}$ is updated as $t_{m,l+1}$. In a similar manner, after the molecular collision treatment, the particle collision time attribute $t_{c,l}$ is reassigned as $t_{c,l+1}$. Once the processes of motion and collision are both completed, the time of the simulation system finally updates from t_l to t_{l+1}.

Similar to the derivation of eq. (5), it is obtained that

$$f(\boldsymbol{c},\boldsymbol{r},t+\Delta t)=[1+(1-\beta)\Delta tJ][1+\beta\Delta tJ] \times[1-(1-\alpha)\Delta tD][1-\alpha\Delta tD]f(\boldsymbol{c},\boldsymbol{r},t)+O[(\Delta t)^2]. \quad (10)$$

The parameters α and β are any constants between 0 and 1. Eq. (9) indicates that the velocity-distributions function $f(\boldsymbol{c},\boldsymbol{r},t+\Delta t)$ is obtained by making the operators $[1-\alpha\Delta tD]$, $[1-(1-\alpha)\Delta tD]$, $[1+\beta\Delta tJ]$ and $[1+(1-\beta)\Delta tJ]$ acting on $f(\boldsymbol{c},\boldsymbol{r},t)$, and the error of this process is as small as the quantity $(\Delta t)^2$. Hence, the particle treatment during a time interval Δt might be divided into four steps. The molecular motion procedure is executed stepwise within two time steps $\alpha\Delta t$ and $(1-\alpha)\Delta t$, while particle collisions are performed in two time steps $\beta\Delta t$ and $(1-\beta)\Delta t$.

Furthermore, eq. (9) is converted into

$$f(\boldsymbol{c},\boldsymbol{r},t+\Delta t)=[1+(1-\beta)\Delta tJ][1-(1-\alpha)\Delta tD] \times[1+\beta\Delta tJ][1-\alpha\Delta tD]f(\boldsymbol{c},\boldsymbol{r},t)+O[(\Delta t)^2], \quad (11)$$

which also shows that the treatments during an interval Δt are of arbitrary sequence.

Actually, a general form might be written as

$$\begin{aligned} &f(\boldsymbol{c},\boldsymbol{r},t+\Delta t)\\ &=[1+\beta_1\Delta tJ][1+\beta_2\Delta tJ]\cdots[1+\beta_M\Delta tJ]\\ &\times[1-\alpha_1\Delta tD][1-\alpha_2\Delta tD]\cdots[1-\alpha_N\Delta tD]f(\boldsymbol{c},\boldsymbol{r},t)\\ &+O[(\Delta t)^2], \end{aligned} \quad (12)$$

where

$$\beta_1+\beta_2+\cdots+\beta_M=1.0,\ \alpha_1+\alpha_2+\cdots+\alpha_N=1.0. \quad (13)$$

In response to the point of molecular movement time attribute and collision time attribute, eq. (12) suggests that the movement time attribute $t_{m,l}$ and collision time attribute $t_{c,l}$ should be updated to $t_{m,l+1}$ and $t_{c,l+1}$, respectively within several fractional steps.

3 Local time stepping algorithm

When the macroscopic gradients vary within wide limits, the appropriate local time steps for different regions of the flow filed are diverse from each other. In order to save computational resources, the local time stepping with self-adaptation is suggested to implement. One of the effective local time stepping schemes was proposed by Laux, which uses a discrete cell-local time step combined with an algorithm for the automatic adaptation [5]. The main idea of this algorithm is that each grid cell is assigned a parameter of time zone $T\in[1,\cdots,T_{\max}]$ of a base time step Δt and at the end of an interval of T time steps, molecular treatments (the molecular motions and collisions) are just preformed. Initially, each cell is assigned the same T_0; as the calculation proceeds, the time zones T are modified based on the local flow conditions [5]. After the adaptations, the time zones T of the grid cells are probably different from each other.

Two parameters might be defined for each grid cell [5]:

$$F(N,T)=\mathrm{mod}(N,T), \quad (14)$$

$$E(N,T)=T-F(N,T), \quad (15)$$

where N is the total number of time steps which the simulation system elapsed. Therefore, F represents the time steps which the corresponding cells have gone through since their last treatments, and E demonstrates the time steps which the cells should wait for from the current moment to the next treatment. Once the condition $F(N,T)=0$ is satisfied, particle treatments are performed within cells and the time of cells are pushed with T steps.

To observe the particles in cell i with time zone T_i, suppose that at the current time step N, the condition $F_i(N,T_i)=0$ is satisfied, and that all the particles within it are treated. Due to the movement, some particles may go to cell j with time zone T_j which is not equal to T_i. The particles, which are still located in cell i, collide then, and the next time step when they will be treated is

$$N_i'=N+T_i. \quad (16)$$

Whereas, for those particles which move to cell j, the next time step they will be treated is

$$N_j'=N+E_j. \quad (17)$$

So, in the imminent treatment, the particles which move to cell j will move and collide according to the same time interval:

$$\Delta t_p=E_j\Delta t. \quad (18)$$

However, since these particles are out of cell i after the movement at time step N, they have no opportunity to collide with the particles which are still in cell i. According to the argument of movement time attribute and collision time

attribute, at the time step N, the movement time attributes of these particles are pushed to $N\Delta t$, but the collision time attributes do not update to $N\Delta t$. As a result, at the time step N_j' when they will be treated in cell j, the collision time interval Δt_c is not equal to Δt_p. This treatment error may have influence on the local collision rate, which is directly dependent on the collision time interval.

To record the movement time attribute t_m and collision time attribute t_c for each molecule can overcome the shortcoming of Laux's scheme mentioned above. For each cell, when the condition $F(N,T)=0$ is satisfied, motion treatments are performed for each particle according to each particle's movement time interval:

$$\Delta t_{m,k} = t - t_{m,k}, \tag{19}$$

where subscript k is the index for particle identification. After the motions, the particles' movement time attributes are updated to the current time. Then, collision treatments are performed among the particles which are in the same cell according to the collision time interval

$$\Delta t_{c,k} = t - t_{c,k}. \tag{20}$$

Similarly, the particles' collision time attributes are updated to the current time after this treatment.

It should be mentioned that the collision time intervals $\Delta t_{c,k}$ of the particles may be different from each other. Since the collision probability between two simulated particles is directly dependent on the time interval $\Delta t_{c,k}$, a little modification should be introduced to the current collision sampling techniques.

Take the NTC method [1] as an example. It is modified such that

$$\frac{n_{\text{cell}}M}{2}(\sigma_T c_r)_{\max}\Delta t_{c,\max}, \tag{21}$$

pairs are selected, and the collision is computed with probability:

$$\frac{\sigma_T c_r}{(\sigma_T c_r)_{\max}}. \tag{22}$$

Then, for the particles in each representative collision pair, the particle parameters are updated with the probability

$$\frac{\Delta t_c}{\Delta t_{c,\max}}, \tag{23}$$

where n_{cell} is the cell number density, M is the total number of particles within a cell, $\Delta t_{c,\max}$ is the maximum collision time interval of the particles within a cell and $(\sigma_T c_r)_{\max}$ is the maximum product of total cross section and relative velocity among the probable collision pairs.

In the automatic adaptation process, the time zone T of a cell is increased or reduced periodically according to the local flow properties. In this study, the criteria on which the adaptation is based are selected as

a. the maximum magnitude of particle velocity $c_{\max}$;

b. the local mean collision rate ν;

c. the maximum number of allowed time zone $T_{\max}$.

The first criterion bases on the requirement that a particle should not cross more than one cell per time step. The second one is the physical nature requirement of DSMC method and the collision rate is calculated as [1]

$$\nu = \frac{4}{\sqrt{\pi}}\sigma_T n_{\text{cell}}\sqrt{\frac{kT_{\text{cell}}}{m}}, \tag{24}$$

where σ_T and m are the total cross section and mass of the molecule, respectively and T_{cell} is the cell temperature. Whereas, the last one is based on the fact that for a large number of time zone, the speedup of the algorithm is not effective [1].

4 Results and discussion

The hypersonic flow over a sphere body is one of the most representative cases for DSMC simulation. Legge and Koppenwallner measured the drag coefficient of the sphere in the hypersonic flows with different Kn numbers under the adiabatic wall condition [10].

In order to test the validity of the proposed local time step scheme, the numerical test was performed under the same condition in ref. [10]. The diameter of the sphere is 0.04 m, and the free flow is nitrogen gas with Mach 9.0 and total temperature 500 K. Five cases of different global Knudsen number were chosen to investigate the drag coefficients of the sphere. The density of the free stream was varied to change the global Knudsen number of the flow as given in Table 1. The Knudsen number was calculated using the sphere diameter as the characteristic length and the variable hard (VHS) sphere model to calculate the mean free path and mean collision time. The conditions of free stream give a wide range of flow regimes from near continuum to rarefied gas flow. In order to satisfy the adiabatic wall condition, the surface of the sphere was fixed the temperature of 500 K.

The DSMC simulations were performed using RGD-tool, a code developed in the authors' group at Beihang University. RGD-tool is a parallel 3-D DSMC code, and it includes vibrational and rotational energy exchange models. In this study, Larsen-Borgnakke models (L-B) were used to deal with the rotational energy exchange of the nitrogen molecular while the vibrational energy was neglected. VHS collision model was also employed.

The scheme using a local time step which specifies the particle motive time attribute and collision time attribute are implemented in RGD-tool. In the structure of the flow about a sphere, there are areas of high gradients, such as the shock

Table 1 Conditions of free flow

Kn_0	P_0 (kg/m^3)	T_0 (K)	V_0 (m/s)
0.01	8.66×10^{-5}	29.1	989.4
0.1	8.66×10^{-6}	29.1	989.4
1	8.66×10^{-7}	29.1	989.4
10	8.66×10^{-8}	29.1	989.4
100	8.66×10^{-9}	29.1	989.4

wave, boundary layer and the areas of rarefied gas flow in the wake. Therefore, the corresponding local time steps vary a lot. On the very beginning, the time zone parameters T for each cell are set to be 1. During the simulations, T can be regulated based on the local macroscopic properties.

The drag coefficient which is presented in this paper is defined as

$$C_D = \frac{F}{\frac{1}{2}\rho_0 u_0^2 S}, \tag{25}$$

where subscript 0 indicates the free flow condition, F is the drag force performed on the sphere, and S is the windward area of the sphere. The simulation results are demonstrated in Table 2. It is seen that in all of the five cases, the relative errors between the simulated results calculated by using RGD-tool and the experimental data are all within ±5%, which demonstrates the validity of the DSMC simulation code RGD-tool.

For detail comparisons, the cases of free flow with Kn=0.1 were calculated using a uniform time step, the Laux's local time stepping scheme and the proposed scheme. Each ran 10000 time steps, and the steady state was reached after about 5000 steps. In all the cases, the based time step was fixed as $\Delta t=10^{-6}$ s and the cell scale was fixed as ΔL=0.001 m. In the uniform-time-step case, the time zones are not changed and always set to be 1. In the other two cases, the maximum time zone allowed was set to be 10 and before the steady status, the time zone adaptation was performed every 500 time steps. For simplification, a fixed particle weight was utilized, and at the end of the simulations, there were about 50 million particles in the flow field.

The drag coefficients are shown in Table 3. It can be figured out that the simulated drag coefficients are in general in good agreement with the experimental ones. The drag coefficient obtained by the program utilizing the proposed local time stepping scheme is larger than the ones obtained by the other two schemes, and more closed to the experimental result.

Table 2 Drag coefficients of the sphere

Kn_0	Simulated drag coefficient	Experimental drag coefficient [10]	Relative error
0.01	1.183	1.139	3.8%
0.1	1.608	1.642	–2.1%
1	2.411	2.440	–1.2%
10	2.585	2.671	–3.2%
100	2.683	2.685	–1.8%

Table 3 Drag coefficients in detail comparison

Case	Kn_∞	Simulated drag coefficient	Experimental drag coefficient [10]	Relative error
Uniform times step	0.1	1.576	1.642	–4.0%
New scheme	0.1	1.608	1.642	–2.1%
Laux's scheme	0.1	1.592	1.642	–3.0%

Figure 1 illustrates the time zone distribution after the flow reached steady state. Two high time-zone regions were obtained in the flow field. The first one came out in front of the sphere. Although the gas density was high in this region, the low gas velocity mainly resulted in the high time-zone value. The second one appeared in the trail of the sphere body. It was mainly because that the local highly rarefied flow had a relatively high local collision time. Comparisons of the average temperature and the pressure contours obtained with the proposed scheme and the Laux's scheme are illustrated in Figures 2 and 3. Comparisons of the average temperature and the pressure contours obtained using the proposed scheme and the uniform time step scheme are also made in Figures 4 and 5. In the figures, the upper half one is the solution of the proposed new scheme and the lower half ones are the solutions of the other two schemes. It is observed in Figures 2 and 3 that the bow shock thickness in front of the sphere is slightly thinner in the solution using the proposed local time stepping scheme. Otherwise, all the solutions are in good agreement.

In Figures 6 to 8, the three solutions are compared in detail along the stagnation line. Figure 6 is comparison of temperatures, Figure 7 is comparison in mass density and Figure 8 is comparison of velocity magnitudes. The solid lines in the figures indicate the different time zones alone the stagnation lines. Flow along this stagnation line can be viewed as a hypersonic flow that passes through a normal shock wave and rapidly decelerates to rest at the wall.

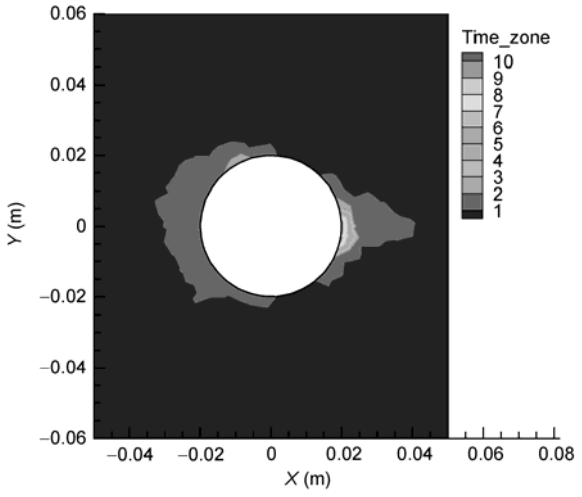

Figure 1 Time zone distribution.

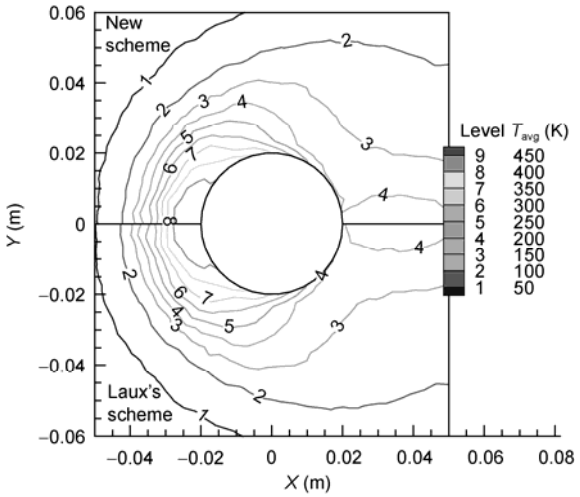

Figure 2 Average temperature comparison of the new scheme solution and the Laux's scheme solution.

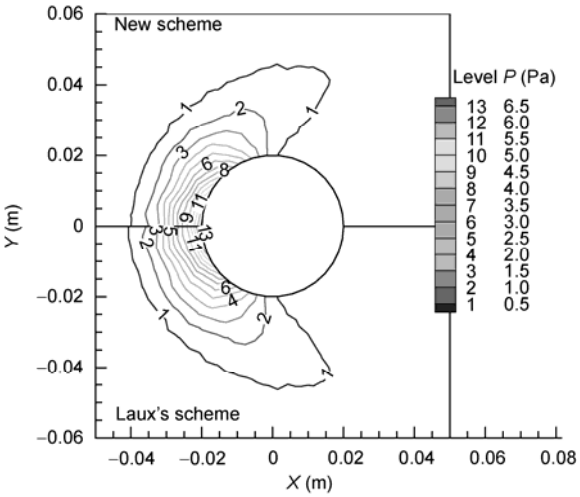

Figure 3 Pressure comparison of the new scheme solution and the Laux's scheme solution.

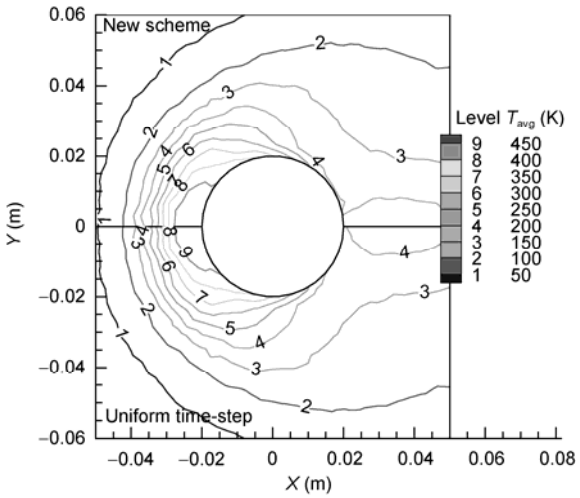

Figure 4 Average temperature comparison of the new scheme solution and the uniform time step solution.

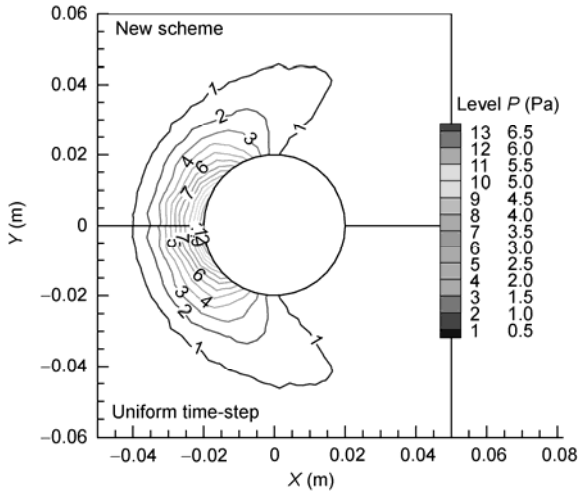

Figure 5 Pressure comparison of the new scheme solution and the uniform time solution.

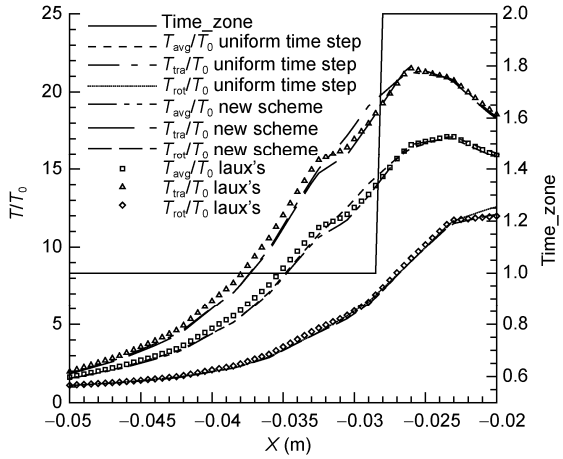

Figure 6 Temperature profiles along the stagnation line.

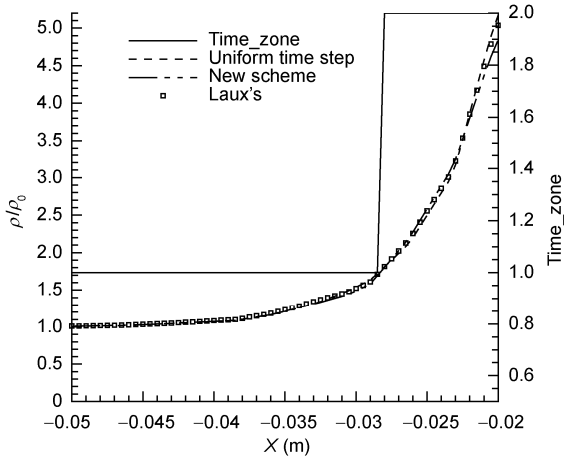

Figure 7 Density profiles along the stagnation line.

Hence, along the line, the flow density and temperature increase, while the gas velocity decreases. The deceleration in

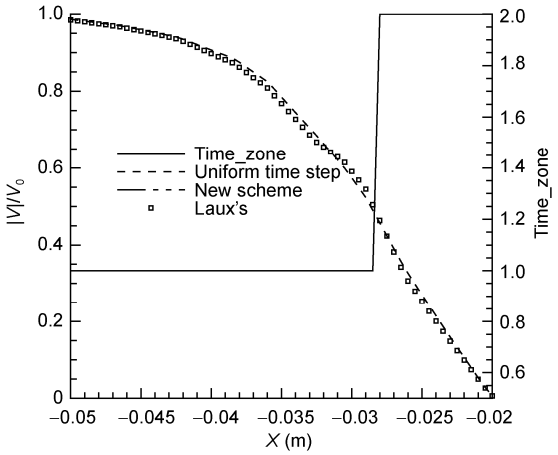

Figure 8 Velocity magnitude profiles along the stagnation line.

velocity mainly results in the increase of time zone. The major differences appear in the translational temperature profiles and the velocity magnitude profiles. Between the solutions of the new scheme and the unit time step, the two profiles are almost in good agreement, expect that a step-sharp discrepancy is observed at the position –0.03 m. However, the same step-sharp tendency also appears in the profile obtained by Laux's scheme at the same position. This behavior is not yet understood and requires further study. On the other hand, the location of initial increase in translational temperature and decrease in velocity magnitude due to the shock wave predicted by the Laux's scheme is slightly upstream the location predicted by the proposed new scheme. The mainly difference between these two solutions appears before the time zone increase from 1 to 2. It might be explained that when the particles pass from the low time-zone region to the high time-zone region, the Laux's scheme overestimates the local collision rates. The relatively high collision rate may reduce the strength of the shock waves.

5 Conclusion

The DSMC method is the most wildly used method for rarefied gas flow simulations. It directly simulates the random evolvement of the particle system to represent the real gas flow. Based on the comprehension of the physic nature, the DSMC method decouples the particle motion and collision which deeply couple in the real gas to simulate the random behaviors of the gas molecules. In this study, from the Boltzmann equation, the foundation of decoupling molecular movement and collision is discussed theoretically. It can be obtained that in DSMC calculations, the molecular motion and collision can be decoupled in a small time interval, and the numerical error this process brings to is as small as the quantity of the time interval squared. Besides, the sequence of motion treatment and collision treatment is arbitrary. Since the particle treatments contain motion and collision, two different time attributes, the movement time attribute and collision time attribute, can be assigned to the simulation particle system. The two time attributes are independent and respectively represent the motion and collision evolvement of the particle system. Only when both the time attributes evolve to a certain time, is the gas flow treated to develop to the same time.

Local time stepping technique with automatic adaptation is used to reduce the computation consumption of the DSMC method. Based on the theoretical discussion above, an improved local time stepping scheme, which specifies the molecular movement time interval and the collision time interval is proposed. This novel scheme may overcome the misestimating of the local collision rate in the published local time step schemes.

Computations of a hypersonic flow about a sphere body are performed to verify the proposed local time stepping scheme and comparisons of the new scheme and a published schemes are also made. The results show that the improved local time scheme is valid. Major differences are observed in flow properties where the local time steps change. The solution of the new scheme obtains a slightly stronger shock wave, which demonstrates that the proposed scheme might be more promising in realizing the flow structure with strong variations.

1 Bird G A. Molecular Gas Dynamics and the Direct Simulation of Gas Flows. Oxford: Clarendon Press, 1994
2 Wilmoth R G, LeBeau G J, Carlson A B. DSMC grid methodologies for computing low-density, hypersonic flows about Reusable Launch Vehicle. In: The 31st AIAA Thermophysics Conference. New Orleans: AIAA, 1996
3 Lumpkin III F E, Fitzgerald S M, Lebeau G J, et al. Study of 3D rarefied flow on a flat plate in the wake of a cylinder. In: The 33rd AIAA Thermophysics Conference. Norfolk: AIAA, 1999
4 Ivanov M S, Markelov G N, Gimelshein S F. Statistical simulation of reactive rarefied flows: numerical approach and applications. In: The 7th AIAA/ASME Joint Thermophysics and Heat Transfer Conference. Albuquerque: AIAA , 1998
5 Laux M. Local Tome Stepping with Automatic Adaption for the DSMC Method. In: The 7th AIAA/ASME Joint Thermophysics and Heat Transfer Conference. Albuquerque: AIAA, 1998
6 Teshima K, Usami M. DSMC Calculation of Supersonic Expansion at a Very Large Pressure Ratio. In: 22nd International Symposium on Rarefied Gas Dynamics. Sydney: AIP conference proceedings, 2001. 737–744
7 Bird G A. The DS2V/3V Program Suite for DSMC Calculations. In: 24th International Symposium on Rarefied Gas Dynamics. Monopoli: AIP Conference Proceedings, 2005. 541–546
8 Shen Q. Rarefied Gas Dynamics (in Chinese). Beijing: National Defense Industry Press, 2003
9 Nanbu K. Direct Simulation scheme derived from the Boltzmann equation. I. monocomponent gases. J Phys Soc Jpn, 1980, 49: 2042–2049
10 Legge H, Koppenwallner G. Sphere Drag Measurement in a Free Jet and a Hypersonic Low Density Tunnel. In: Rarefied Gas Dynamics VII symposium. Pisa: Tecnico Scientifica, 1970. 1: 481–488